Measurement of flame temperature and adiabatic burning velocity of methane/air mixtures

Combust. Sci. and Tech., 1994, Vol. 96, pp. 327-344
Photocopying permitted by license only

Measurement of Flame Temperature and Adiabatic Burning Velocity of Methane/Air Mixtures

A. VAN MAAREN, D. S. THUNG, L. P. H. DE GOEY *Eindhoven University of Technology Faculty of Mechanical Engineering (W-Hoog 3.116) P. O. Box 513, 5600 MB Eindhoven The Netherlands*

(Received June 8, 1993; in final form September 27, 1993)

Abstract—A simple and accurate method is presented to determine the flame temperature and the adiabatic burning velocity of laminar premixed flat flames, using a specially constructed flat flame burner. The heat loss of the flat flame is determined from measurement of the temperature profile of the burner plate. The adiabatic burning velocity is found when the burner plate temperature profile is uniform, implying that the net heat loss of the flame is zero. Several methods are presented to determine the thermal conductivity of the burner plate. The results for methane/air mixtures are compared with experimental data found in the literature and one-dimensional flame calculations, and close agreement is found. The method is particularly useful in providing an accurate reference for other temperature measurement techniques (e.g. spectroscopic laser diagnostics), and to determine adiabatic burning velocities over the entire range of flammability.

Key words—flat flames, flame temperature, adiabatic burning velocity

LIST OF SYMBOLS

A, a, b, C	constant	arbitrary units
c_p	specific heat at constant pressure	$m^2 .s^{-2}.K^{-1}$
d	burner plate perforation diameter	m
h	burner plate thickness	m
J_0	zero order Bessel function	-
l	burner plate perforation pitch	m
$\dot{m}$	mass flow rate	$kg.m^{-2}.s^{-1}$
q	heat flow rate	$kg.s^{-3}$
Q	heat flow rate	$kg.m^2.s^{-3}$
r, R	radius	m
S_L	adiabatic burning velocity at 298 K	$m.s^{-1}$
t	integration variable	K
T	temperature	K
u	(gas) velocity	$m.s^{-1}$
x, y	spatial coordinate	m
α	heat transfer coefficient	$W.m^{-2}.K^{-1}$
θ	geometrical angle in the burner plate	deg
ε	geometrical constant	-
ϕ	equivalence ratio	-
λ	thermal conductivity	$kg.m.s^{-3}.K^{-1}$
ρ	mass density	$kg.m^{-3}$
ξ	burner plate porosity	-

Super- and subscripts

$'$	non-adiabatic
$-$	average
$_b$	burnt gas
$_{br}$	solid brass

g	(unburnt) gas
p	burner plate
r	radial direction
x	axial direction
0	initial
1,2,3,4	thermocouple positions

INTRODUCTION

In recent years large progress has been made in the prediction of temperature and species concentration distributions in laminar gas flames. Much can be attributed to the development of complex chemistry flame codes and transport models. Much effort has been made to determine the elementary reaction rate coefficients. However, in some cases the experimental error with which these coefficients are determined is relatively large. This necessitates fitting of some important reaction rate coefficients with experimental data of adiabatic burning velocities (Warnatz and Chevalier, 1993). Unfortunately, there exists large scatter in the values of adiabatic burning velocities reported in the literature. Therefore it is necessary to perform more research concerning adiabatic burning velocities.

Perhaps the most used technique to measure the adiabatic burning velocity is the opposed jet method (see e.g. Wu and Law (1984), Law (1993)). A major disadvantage of this method is that the adiabatic burning velocity is found by linear extrapolation of the results to zero stretch rate. This linear extrapolation may result in an overestimation of the burning velocity of maximum 10% (Law, 1993).

Another technique is the closed vessel method. The adiabatic burning velocity is found by extrapolation of time-pressure recordings (Lewis and von Elbe, 1961). Also optical techniques to monitor the flame front position and measurement of the unburnt gas velocity are employed (Andrews and Bradley, 1972). Corrections should be made for stretch in all cases. Furthermore, the influence of gravitation may affect the results as well (Clarke *et al.*, 1993).

There are a number of other techniques that will not be discussed here, since it is not our aim to give an extensive review. However, it is clear that a method for measuring the adiabatic burning velocity without a necessary correction for stretch and without any extrapolation, has large advantages compared to the mentioned techniques.

Besides modelling of laminar gas flames, sophisticated "laser diagnostics" have also greatly contributed to the increase in understanding of the complex phenomena in gas flames. These techniques produce detailed information on species concentration and temperature distributions in flames. Large advantage of these techniques is that they are non-intrusive. However, most temperature methods yield only qualitative results, for instance when quenching is important, or they incorporate a relatively large experimental error because of a low signal strength. If an absolute reference temperature measurement would be available, or an accurate calibration, some of these problems could be solved.

In this paper a specially designed flat flame burner is introduced. With this burner the flame temperature T_b' and the adiabatic burning velocity S_L can be determined easily and accurately, by measuring the heat loss q of the flame with small thermocouples attached to the burner head plate. T_b' is determined by subtracting this heat loss from the enthalpy of an adiabatic flame. Since the adiabatic flame temperature T_b (calculable with an error of only a few degrees) is used as reference, the error in T_b' is small. S_L is found by adjusting the unburnt gas velocity until zero heat loss is found.

This method is similar to the method described by Botha and Spalding (1954), who determined the heat loss of flames stabilized on a porous plug burner by measuring the temperature rise of the cooling water. However, the temperature rise of the cooling

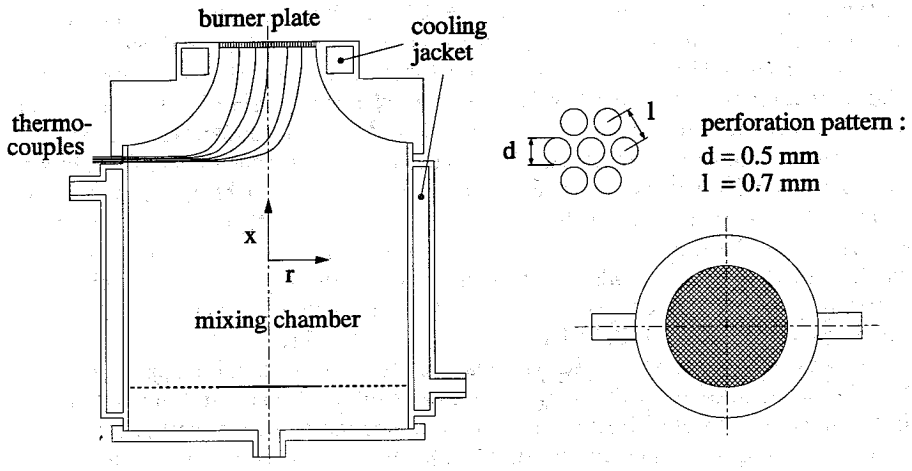

FIGURE 1 The perforated plate burner.

water is small, and it is assumed implicitly that the heat loss from the flame to the burner is uniform over the entire burner surface. Furthermore, the adiabatic burning velocity is found through extrapolation to zero heat loss of the flame to the burner.

The method presented here is accurate, and it is possible to study to what extent the flame temperature distribution is uniform. The uniformity of the heat loss across the burner plate can be determined by examining the burner plate temperature distribution. Furthermore, by using a perforated plate instead of a porous plug as stabilizing surface, Laser Doppler Velocimetry measurements are possible in both the unburnt gas flow (without a flame) and in the burnt gas flow. This is employed to determine the uniformity of the flow velocity distributions as well. Besides, the adiabatic burning velocity is found without extrapolation to zero heat loss, and without correction for stretch.

With the new flat-flame burner a well-defined flame is created, with a well-known flame temperature and burning velocity. The method is most accurate when the flame is near-adiabatic. It therefore can provide a reference for other, detailed temperature measurement techniques. Versluis (1992) used the method to determine OH-predissociation rates, necessary to perform quantitative temperature measurements in flames with a Laser Induced Predissociation Fluorescence technique. Furthermore, the results found for S_L can be employed to contribute to the validation of chemical reaction schemes.

One aspect of methods using a flat flame burner, that has not been clarified yet, is the possibility of radical recombination at the burner surface. Since the burning velocity is very sensitive to composition changes, this may affect the measurement results. Eng *et al.* (1991) performed a numerical study on some radical recombination effects, but found no significant influence. However, their study was limited, and therefore more research is necessary to be able to exclude this kind of problems.

THE PERFORATED PLATE BURNER

In figure 1 the rotationally symmetric flat flame burner is shown. It consists of a burner head with a cooling jacket, mounted on a mixing chamber. The latter also serves to provide uniform flow inside the burner head. The mixing chamber is cooled separately from the burner head with cooling temperature equal to room temperature of 298 K.

The most important part of the burner is the burner plate. This is a brass plate of radius $R = 15$ mm and plate thickness $h = 2.0$ mm, perforated with a hexagonal pattern

of small holes of $d = 0.5$ mm diameter and $l = 0.7$ mm pitch. Two-dimensional numerical calculations with one-step chemistry, performed in our group with the flame code of De Lange and De Goey (1993), have shown that for holes smaller than 0.55 mm diameter and burning velocities up to 0.5 m/s flame curvature on the scale of the holes does not appear. Local stretch can therefore be excluded. Local flame temperature variations do also not arise. Effectively the flame is almost perfectly one-dimensional (1-D). However, for hole diameters larger than 0.55 mm, flame curvature and flame temperature variations are found. This leads to the conclusion that to obtain a 1-D flame, only a perforation hole diameter of 0.5 mm or less may be used. Presently we are also investigating the application of the burner to higher burning velocities than 0.5 m/s. For high burning velocities (e.g. 1-2 m/s Hydrogen flames), turbulence cannot be excluded. In that case the diameter of the holes of the perforation should be reduced.

At the upstream side of the burner plate a number of small Copper/Constantan thermocouples is soldered inside holes of the perforation. Since one hole is blocked by each thermocouple, local distortion of the flow is inevitable. To reduce the effect on the measurements to a minimum, the thermocouples that are used are very thin (0.1 mm). Then the distortion of the unburnt gas velocity is restricted to a negligibly small area around each thermocouple. The thermocouple wires are insulated to prevent heat loss to the unburnt gas and electrical contact with the burner wall (see figure 1). The wires inside the burner did not appear to cause any observable distortion of the flow pattern.

Boundary layers exist near the edges of the burner, due to the influence of the environment. In these regions the flame will not be flat. Therefore, the thermocouples are located in an area where these boundary layer effects are negligible, the 1-D area. For the burner shown in figure 1 the 1-D area is defined by the region around the centerline with $r < 12$ mm. The magnitude of this area is determined by means of Laser Doppler Velocimetry measurements in both the unburnt and the burnt gas flow. Apart from the small velocity distortions induced by the thermocouples, the unburnt gas velocity distribution varies only about 1% inside the 1-D area (Van Maaren and De Goey, 1993).

Due to the velocity boundary layers, the average unburnt gas velocity u_g within the 1-D area (which is equal to the burning velocity) differs from the average gas velocity set by mass flow controllers. Consequently, the actual burning velocity inside the 1-D area must be determined by Laser Doppler Velocimetry for each value of the mass flow rate.

STABILIZATION OF FLAT FLAMES

It is well known the flames are stabilized on flat flame burners mainly by heat loss to the burner, if the unburnt gas velocity u_g is below S_L. In the first instance the burner surface temperature is irrelevant for the flame temperature, which is determined only by the initial conditions of the gas mixture (temperature, pressure and composition). However, when the surface temperature shows large variations, the velocity and temperature distribution of the unburnt gas may be seriously distorted (Kihara *et al.*, 1975). This may affect the temperature distribution of the flame. Therefore it is essential to apply some kind of cooling to the burner, in order to minimize the burner surface temperature differences. When a porous plug burner is used, which has a relatively low thermal conductivity, both cooling of the edge of the plug and the inside of the plug must be applied to meet with this requirement. However, the thermal conductivity of the perforated plate burner, used in this study, is high enough to make internal cooling unnecessary. The perforation pattern and the thickness of the burner plate are chosen in such a way, that the resulting maximum radial temperature difference across the plate (within the 1-D area) is about 20 K. This can be measured accurately with thermocouples, while it will

have a negligible effect on the flame. Laser Doppler Velocimetry measurements have shown, that the maximum distortion of the velocity distribution of the burnt gas is only a few percent, inside the 1-D area (Van Maaren and De Goey, 1993). Besides, if O (10) K radial temperature variation would be present in the gas as well, then the ratio of heat transport in axial and radial direction is:

$$\frac{-\lambda_g \partial^2 T_g/\partial x^2}{-\lambda_g \partial^2 T_g/\partial r^2} \approx \frac{\Delta T_{g,x}[\Delta r]^2}{\Delta T_{g,r}[\Delta x]^2} \approx \frac{10^3 \cdot [10^{-2}]^2}{10 \cdot [10^{-3}]^2} \approx O(10^4) \tag{1}$$

in which λ_g is the heat conductivity and T_g the temperature of the gas. Heat transport in radial direction is four orders of magnitude smaller than heat transport in axial direction. Therefore, radial temperature variations in the burner plate of O (10) K will have a negligible influence on the flame.

Although the temperature at which the burner plate edge is fixed by the cooling water is irrelevant to the flame temperature, applying a high cooling water temperature increases the stability of the flame. If the temperature of the cooling water is equal to the unburnt gas temperature, the flame will blow off or become distorted at burning velocities near the adiabatic value. As reported by De Goey *et al.* (1993) it is possible to stabilize flat adiabatic flames if the temperature of the cooling water is well above the unburnt gas temperature. This principle is used in the determination of S_L. The cooling water temperature for all experiments was 368 K.

THE FLAME TEMPERATURE

To be able to determine the flame temperature, a relation has to be found between T_b' and the measured burner plate temperature distribution. When a flame is stabilized above the burner plate, the energy equation for the burner plate inside the 1-D area (in cylindrical coordinates) can be written as:

$$-\frac{\partial}{\partial x}\left[\lambda_{p,x}(r)\frac{\partial T_p(x,r)}{\partial x}\right] - \frac{1}{r}\frac{\partial}{\partial r}\left[\lambda_{p,r}(r) r \frac{\partial T_p(x,r)}{\partial r}\right] = \alpha(x)[T_g(x,r) - T_p(x,r)] \tag{2}$$

In this equation is T_p the temperature of the plate, T_g the temperature of the gas, $\lambda_{p,x}$ and $\lambda_{p,r}$ the thermal conductivity of the burner plate in axial and radial direction, respectively, and α the coefficient of heat transfer between the gas and the burner plate.

Tangential contributions are omitted in (2) because of rotational symmetry of the flow, and because $\lambda_{p,r}$ is very nearly isotropic, despite the fact that the perforation pattern is non-isotropic (we will return to this point later).

Integration of (2) over the burner plate thickness, from $x = 0$ to $x = h$, gives:

$$-\frac{1}{r}\frac{\partial}{\partial r}\left[\lambda_{p,r}(r) r \frac{\partial}{\partial r}\int_0^h T_p(x,r)dx\right] = \int_0^h \alpha(x)[T_g(x,r) - T_p(x,r)]dx + \lambda_{p,x}\frac{\partial T_p}{\partial x}|_{x=h} - \lambda_{p,x}\frac{\partial T_p}{\partial x}|_{x=0} = q(r) \tag{3}$$

In this equation, q is the *net* heat transfer from the gas to the plate, including the heat loss of the flame and the heat gain of the unburnt gas. q is independent of r in the case of a 1-D flame. The average plate temperature $\bar{T}_p(r)$ is defined by:

$$\bar{T}_p(r) = \frac{1}{h}\int_0^h T_p(x,r)dx \tag{4}$$

$\bar{T}_p$ substituted in (4) yields:

$$-\frac{1}{r}\frac{d}{dr}\left[\lambda_{p,r}(r)r\frac{d\bar{T}_p(r)}{dr}\right] = \frac{q(r)}{h} \tag{5}$$

This equation is only dependent on r, giving a relation between the net heat loss of the flame and the plate temperature distribution.

$\lambda_{p,r}$ cannot be taken temperature independent in the range of plate temperatures occurring during the measurements. Using experimental data of Bode and Fritz (1954) and DIN Taschenbuch 26 (1984), the heat conductivity of solid brass λ_{br} is approximated by a linear function of temperature:

$$\lambda_{br}(T) = a + b \cdot T \tag{6}$$

with constants $a = 73.1\ \mathrm{W.m^{-1}.K^{-1}}$ and $b = 0.160\ \mathrm{W.m^{-1}.K^{-2}}$. Because of the perforation of the burner plate $\lambda_{p,r}$ is considerably smaller than λ_{br}. As this is only a geometrical effect, $\lambda_{p,r}$ is regarded as being the product of λ_{br} and a constant ε:

$$\lambda_{p,r}(T) = \varepsilon \cdot \lambda_{br}(T) \tag{7}$$

The value of ε depends on the diameter and pitch of the holes of the perforation.

The measurement of the average plate temperature $\bar{T}_p$ with thermocouples requires that the maximum temperature variation in axial direction inside the burner plate $\Delta T_{p,x}$ is small. This can be estimated by the following argument. As λ_g is much smaller than $\lambda_{p,x}$, we assume that any heat flux in axial direction is entirely conducted through the burner plate, and not through the gas. Furthermore, it can be shown that, due to the high heat transfer coefficient α, the gas inside the burner plate attains practically the same temperature as the burner plate. For $x \to -\infty$ to $x = 0$ (at the upstream side of the burner plate), conservation of energy in the unburnt gas yields:

$$\dot{m}c_pT_g^0 = \dot{m}c_pT_g - \lambda_g\frac{\partial T_g}{\partial x} \tag{8}$$

with $\dot{m} = \rho_g u_g$ the mass flow rate, c_p the specific heat and T_g^0 the initial temperature of the unburnt gas. At $x = 0$, the conductive term on the right-hand side of (8) equals the axial conductive heat flux inside the burner plate. With $T_g \approx T_p$ inside the burner plate this leads to:

$$\dot{m}c_p[T_p - T_g^0] = \lambda_{p,x}\frac{\partial T_p}{\partial x} \approx [1-\xi]\lambda_{br}\frac{\Delta T_{p,x}}{\Delta x} \tag{9}$$

with ξ the porosity of the burner plate, defined by:

$$\xi = \frac{\pi}{2\sqrt{3}}\left[\frac{d}{l}\right]^2 \tag{10}$$

With a typical temperature difference $T_p - T_g$ of 100 K, evaluation of (9) yields an estimate for $\delta T_{p,x}$

$$\Delta T_{p,x} \approx \frac{\dot{m}c_p[T_p - T_g^0]\Delta x}{[1-\xi]\lambda_{br}} \approx \frac{1\cdot 10^3 \cdot 10^2 \cdot 10^{-3}}{1\cdot 100} \approx O(1)K \tag{11}$$

This shows that axial temperature variations inside the burner plate are negligible compared to the radial temperature variations (maximum 20 K), and that the thermocouple measurement results of $\bar{T}_p$ will possess only a small error due to these variations. Now, q can be determined by (5), (6) and (7). A relation between T_b' and q is still needed. If for a given gas mixture T_b is know, this relation can be written as:

$$q = \dot{m} \int_{T_b'}^{T_b} c_p(t) dt \tag{12}$$

The combination of (5), (6), (7) and (12) constitutes an implicit equation for T_b'. Since (12) is an integration of the energy equation of the gas from $x = h$ (the burner plate surface) to $x \to \infty$, downstream heat loss in the main flow direction is incorporated. Heat loss in radial direction perpendicular to the main flow is not incorporated, but will be negligibly small if the burner diameter is large enough.

With (12) the accuracy of T_b' is, among others, dependent on the accuracy with which T_b is determined, in particular, the accuracy with which the burnt gas composition can be known. However, it is our opinion that this can be performed with a small error, when realistic assumptions concerning the chemical equilibrium composition of the burnt gas are made. Therefore we believe that this requirement is not a real problem.

Through integration of (5) an analytical solution for the plate temperature distribution can be obtained:

$$\bar{T}_p(r) = -\frac{a}{b} + \left[\frac{q[R^2 - r^2]}{2hb\varepsilon} + \left[\frac{a}{b} + T_R\right]^2\right]^{\frac{1}{2}} \tag{13}$$

where $T_R = \bar{T}_p(R)$ is used as boundary condition. The procedure to determine T_b' is to measure the burner temperature $\bar{T}_p$ at various radii r, and to determine q with a least square fit of the thermocouple measurement data to (13). Deviations from uniformity of the distribution of q can be estimated from the standard deviation of q. Finally T_b' is found by iteration using (12).

THE GEOMETRICAL CONSTANT ε

An important parameter in (13) is the geometrical constant ε. Its value must be determined accurately to be able to perform accurate temperature measurements. Therefore several methods have been used to determine ε, which will be treated here.

Additional data for ε have been obtained for an older version of the burner. Therefore these results are shown here as well. The geometrical parameters of the burner plate of this particular burner are: $R = 14$ mm, $d = 0.4$ mm, $l = 0.5$ mm, and $h = 1.85$ mm. Compared to the old burner, improvements in the new burner design are the cooling of the mixing chamber (to keep the unburnt gas mixture at room temperature before flowing through the burner head), and the reduction of the temperature differences across the burner plate to a maximum of 20 K by taking larger values of both h and ε.

Analytical And Numerical Methods

Perrins *et al.* (1979) considered the conductivity of a hexagonal matrix of cylinders embedded in a solid medium. The conductivity of the solid medium is set equal to one, and that of the cylinders equal to zero (in this case, since air may be regarded as a perfect insulator compared to solid brass). The overall heat conductivity of one unit cell of the matrix is then equal to ε. In figure 2 the situation is shown. Important to realize is that

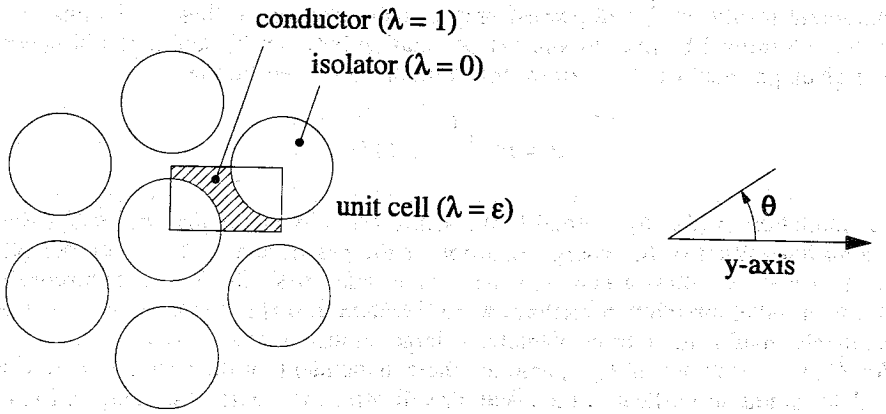

FIGURE 2 The hexagonal pattern of conducting cylinder.

TABLE I
The Geometrical Factor ε of the Thermal Conductivity of the Burner Plate; $\theta = 0°$ Corresponds to the y-direction (see Figure 2)

	d = 0.4 mm, l = 0.5 mm		d = 0.5 mm, l = 0.7 mm	
	ε [-]	error [%]	ε [-]	error [%]
Perrins *et al.* 1979				
$\theta = 0°$	0.264	$\ll 1$	0.362	$\ll 1$
$\theta = 30°$	0.264	$\ll 1$	0.362	$\ll 1$
Sonnemans (1992)				
$\theta = 0°$	0.262	1	0.362	1
$\theta = 10°$	0.263	1	0.362	1
$\theta = 20°$	0.264	1	0.362	1
$\theta = 30°$	0.264	1	0.362	1
Experimental				
heat sink method	0.266	7	0.369	3
heat source method	0.255	4		
Van Maaren, Thung and De Goey (1994)				

ε may vary with the direction in which heat transport is considered, since the matrix is non-isotropic for conductive transport in different directions. With the method described by Perrins *et al.*, ε can be determined only for heat transport in two specific directions, due to the restrictions imposed on the method by application of the periodical boundary conditions. The first direction corresponds to angles with the y-axis shown in figure 2 of $\theta = 0°, 60°, 120° \cdots$, the second to angles $\theta = 30°, 90°, 150° \cdots$.

In table 1 the results of the calculations for the perforation pattern of both perforated plate burners are presented. It appears that there is practically no difference in ε between $\theta = 0°$ and $\theta = 30°$, for both burner plate geometries.

To investigate the variation of ε for other values of θ, the heat conduction problem in arbitrary direction has been solved numerically by Sonnemans (1992). The same matrix was taken, but now by choosing different boundary conditions, and several unit cells as calculation domain, θ could be set to any desired value. In table 1 some results are presented for both the 28 mm and the 30 mm burner. For $\theta = 0°$ and 30°, the differences between results of Perrins *et al.* and Sonnemans are well within the numerical error of 1%. Furthermore, it appears that the variation of ε for different directions is not significant. Only when the matrix is very dense, i.e. when the cylinder diameter-pitch ratio d/l approaches unity, differences are found that cannot be neglected.

Experimental Methods

The manufacturing of the burner plate can result in small differences in hole diameter, and also irregularities such as burrs are possible. To investigate their effect on $\lambda_{p,r}$, and to validate the calculated results of ε, two different experimental approaches to determine $\lambda_{p,r}$ have also been explored, to be treated next.

The heat sink method An air flow at room temperature is forced through the burner plate with cooling water temperature set to a high value (e.g. 368 K). The radial temperature distribution is measured with the thermocouples attached to the burner plate. In this case the energy equation for the burner plate can be written as:

$$-\frac{1}{r}\frac{d}{dr}\left[\lambda_{p,r}(r) r \frac{d\bar{T}_p(r)}{dr}\right] = \frac{\dot{m} c_p}{h}[T_g(h,r) - T_g(0,r)] \tag{14}$$

where $T_g(x,r)$ is the temperature of the gas at axial position x inside the burner plate, with $x = 0$ at entrance. We assume that $\dot{m}$ is constant as well as c_p.

If it is also assumed that $\lambda_{p,r}$ is constant, that $T_g(0,r) = T_g^0$ (the air temperature distribution at the upstream side of the burner plate $x = 0$ is uniform) and that $T_g(h,r) = \bar{T}_p(r)$ (the air temperature at $x = h$ equals the local burner plate temperature $\bar{T}_p(r)$), then an analytical solution is known:

$$\bar{T}_p(r) = C \cdot J_0(A \cdot r) + T_g^0$$

$$\text{with } A = \left[\frac{\dot{m} c_p}{\lambda_{p,r} h}\right]^{\frac{1}{2}} \tag{15}$$

where J_0 is the zero order Bessel function. The constant C as well as ε can be found by substituting twice a measured value for the plate temperature, at two different radii r_1 and r_2.

It appears that using (15) yields reliable results only for $u_g < 0.25$ m/s. The explanation for this is that the assumption $T_g(h,r) = \bar{T}_p(r)$ is not valid for higher gas velocities. Then the air cannot be heated up completely to the same value as the $\bar{T}_p(r)$, since the Nusselt number for laminar flow in a tube is practically independent of Reynolds number (Bird *et al.*, 1960). Therefore, with increasing gas flow the amount of heat transferred from the plate to the gas does not increase.

In (15) only two thermocouple measurements are used, which makes the result rather sensitive to experimental errors. Therefore (14) is also solved numerically with $\dot{m}$ now varying according to Laser Doppler Velocimetry measurements, and with $\lambda_{p,r}$ varying

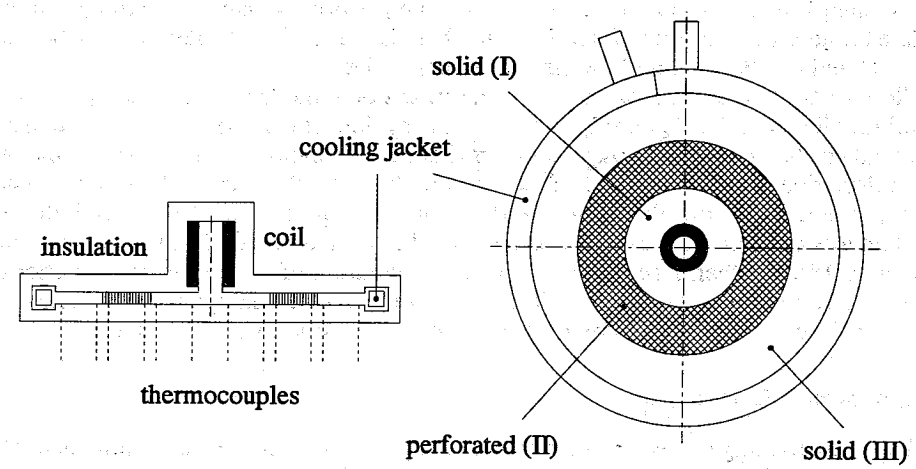

FIGURE 3 The experimental setup of the Heat Source Method.

with temperature according to (6). ε is found by fitting the temperature measurements of all the thermocouples to the numerical solution of (14). Air velocities are restricted to the range 0.10-0.25 m/s. Decreasing the velocity below 0.10 m/s results in temperature differences across the burner plate which are too small to yield accurate results for ε.

The results for ε for both burners are presented in table 1. It appears that the calculated values for ε obtained with the analytical and numerical methods are confirmed within an experimental error of 3 and 7%.

The heat source method The second experimental method employs a specially designed "burner" plate, shown in figure 3. In the center of a thin plate a heating coil is attached to a brass rod, to apply a heat flow to the plate. The plate has three annular regions: two regions of solid brass (I, III), and an intermediate part with the same perforation pattern as the burner plate (II), with $d = 0.4$ and $l = 0.5$ mm. The edge of the plate is maintained at a constant temperature (293 K) by means of a cooling jacket. Thermocouples are attached to the plate at various radii and angles, and the entire plate is insulated to prevent heat loss to the environment. Conservation of energy can be written as:

$$-\frac{1}{r}\frac{d}{dr}\left[\lambda_{p,r}(r) r \frac{d\bar{T}_p(r)}{dr}\right] = 0 \tag{16}$$

This equation is only valid for radii larger than the radius of the brass rod with the heating coil. Because heat losses to the environment are negligible, the total radial heat flow Q through the plate is constant throughout the entire plate. Integration of (16) yields:

$$\lambda_{p,r}(r)\frac{d\bar{T}_p(r)}{dr} = -\frac{Q}{2\pi r h} \tag{17}$$

In both massive regions of the plate $\varepsilon = 1$, so Q can be found by measuring $T_1 = \bar{T}_p(r_1)$ and $T_2 = \bar{T}_p(r_2)$ in either massive regions. With Q known, ε can be found by measuring $T_3 = \bar{T}_p(r_3)$ and $T_4 = \bar{T}_p(r_4)$ in the perforated region by integrating (17) once more:

$$\varepsilon = \frac{Q \ln\left(\frac{r_3}{r_4}\right)}{2\pi h\left[a \cdot [T_4 - T_3] + \frac{1}{2}b \cdot [T_4^2 - T_3^2]\right]} \tag{18}$$

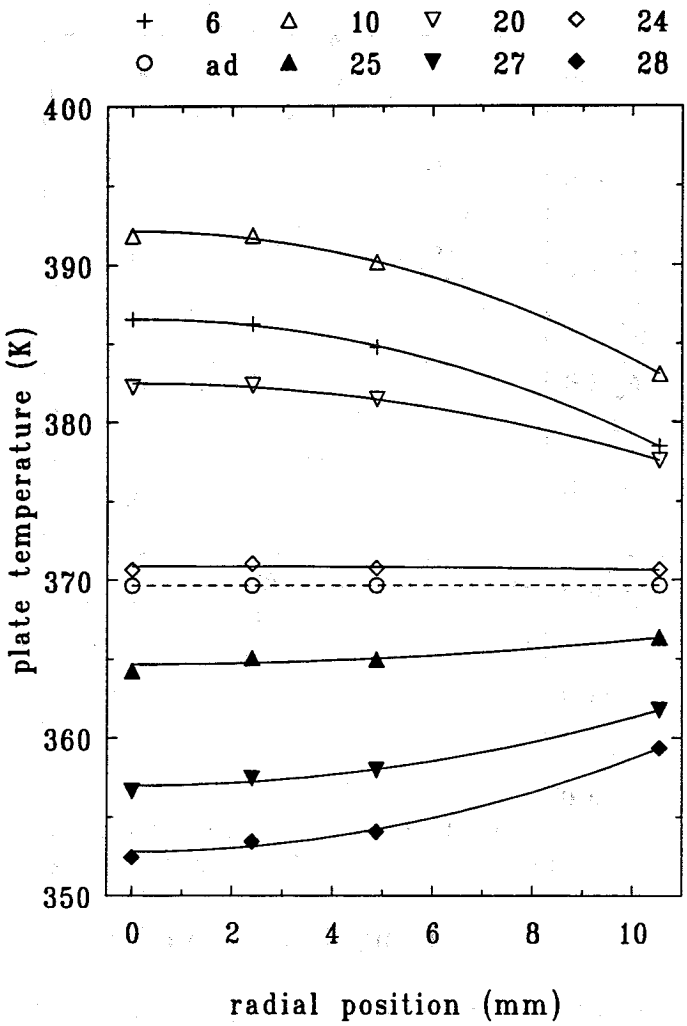

FIGURE 4 The measured burner plate temperature distribution; $\phi = 0.8$, burning velocity 0.06-0.28 m/s; markers: measurements, lines: fit.

In table 1 the results are presented. Now the calculated values are confirmed with an error of about 4%. In this error any difference that was found when using thermocouples at different angles is included.

The numerical work of Sonnemans and both experimental methods agree well with the results of the analytical equation given by Perrins *et al.* for ε. Also it is confirmed that there is no significant tangential dependence in ε, so that ε may be treated as being isotropic. Considering all the available data on ε, the calculated value of Perrins will be used, with an uncertainty of about 3% due to possible manufacturing irregularities in the perforation pattern.

RESULTS

In figure 4 an example of results for the burner plate temperature distribution is shown,

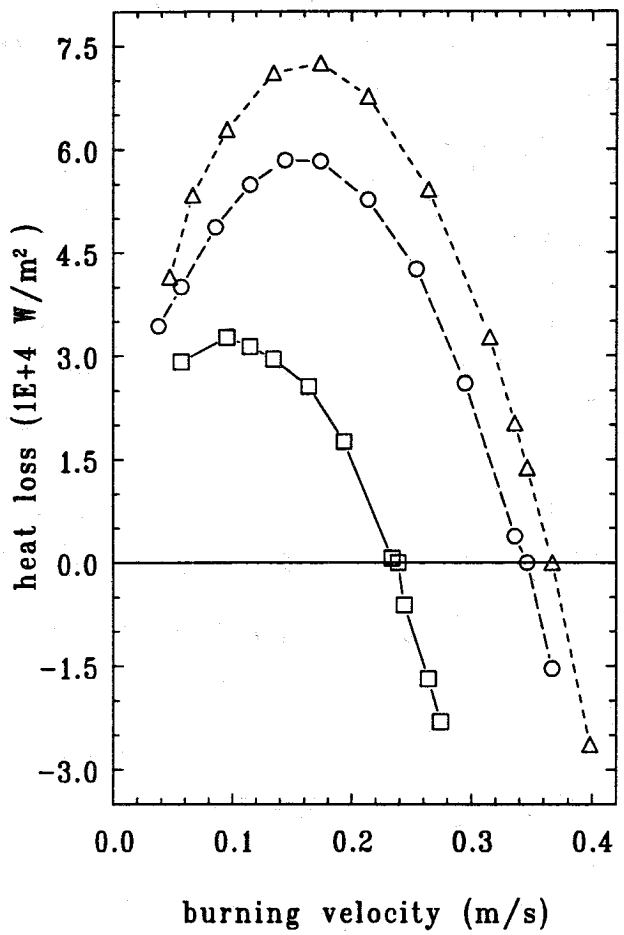

FIGURE 5 The calculated heat loss to the burner for $\phi = 0.8$ (square markers), 1.0 (triangle markers) and 1.2 (circle markers).

for a methane/air mixture with equivalence ratio $\phi = 0.8$. Note that the 1-D area extends beyond the position of the outer thermocouple. The markers denote the measurements, while the continuous lines denote the fit using (13). The accuracy of the thermometer device was 0.1 K. However, the reproducibility of the plate temperature appeared to be about 0.3 K. As the maximum temperature differences between the fit and the measurements are about 0.5 K, these results confirm the assumption of taking q constant.

The results in figure 4 with a negative slope of the plate temperature correspond to $u_g < S_L$. The uniform temperature profile for $u_g = S_L$ is also shown (denoted by $ad.$). The results showing a positive slope of the temperature profile correspond to $u_g > S_L$. Here the heat loss of the flame was smaller than the heat gain of the unburnt gas from the hot burner plate. Nevertheless, the flame remained perfectly flat, as long as u_g did not exceed S_L too much. However, a further increase of u_g caused (partial) blow off.

In figure 5 is shown q as function of the burning velocity, for $\phi = 0.8$, 1.0 and 1.2. An estimate of the uniformity of the q distribution is obtained, considering the standard

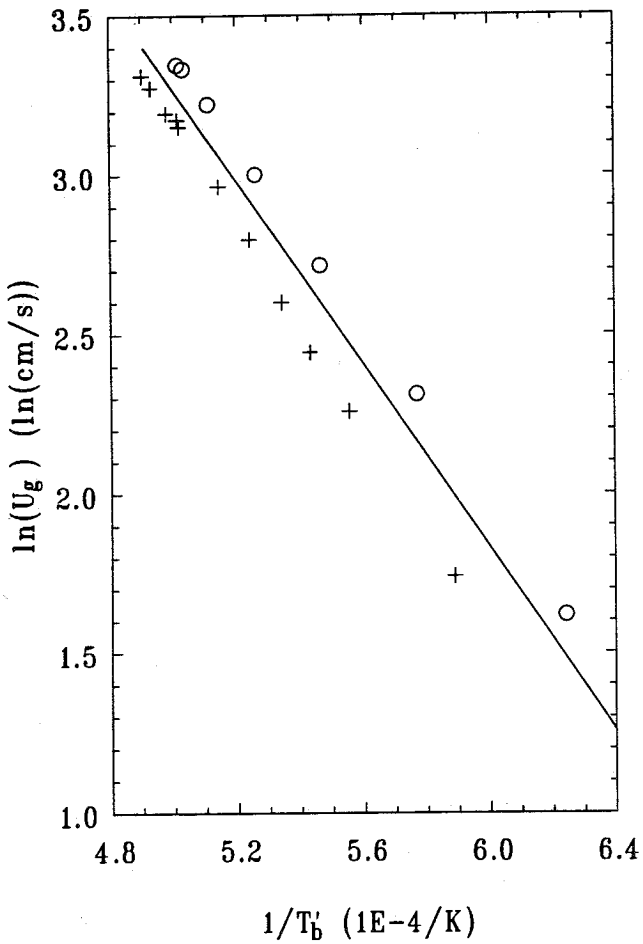

FIGURE 6 Flame temperature versus burning velocity for $\phi = 0.8$; cross markers: measurements, circle markers: calculations, continuous line: Kaskan (1959).

deviation of the burner plate temperature fit. It appears that for high values of q the error is 1-5%, increasing to 10% or more for low values of q. However, the latter is caused by the increasing experimental error due to the decreasing temperature differences over the burner plate. Therefore these results also confirm the assumption of taking q constant.

The negative values of q for $u_g > S_L$ are also shown. At intersection with the horizontal axis of figure 5 the value of S_L is found.

In figures 6 to 8 the results for the flame temperature are presented. To validate these results a comparison is made with both experimental results found in literature and 1-D flame calculations. Experimental data are obtained from Kaskan (1959), who presented a compilation of measurements presented in the literature, using different measurement techniques. An experimental fit of these measurements determined by Kaskan is also shown in figures 6 to 8. The 1-D flame calculations are performed with the code of Kee *et al.* (1991). The (C_1) chemical reaction mechanism that has been used consisted of 58 reactions between 17 species, and was the same as described by Kee *et al.* (1991). The

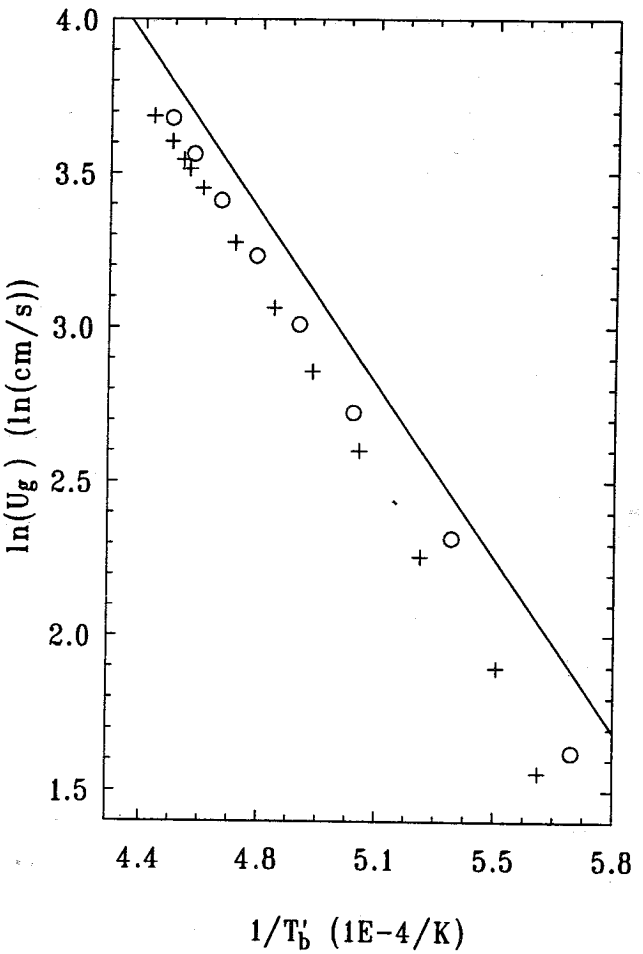

FIGURE 7 Flame temperature versus burning velocity for $\phi = 1.0$; cross markers: measurements, circle markers: calculations, continuous line: Kaskan (1959).

thermodynamic properties and the transport model coefficients were taken according to Kee *et al.* (1986, 1987). These results are also plotted in figures 6 to 8. It is shown that good agreement is obtained, although there is a systematic difference. The difference with the experimental data of Kaskan can be explained by the fact, that Kaskan finds different values for T_b. The values for T_b that have been used are derived from adiabatic 1-D flame calculations. If the values for T_b of Kaskan are used for the calculation of T_b', the results agree within about 30 K. The differences between the experimental results and the 1-D flame calculations are of the same order of magnitude as when compared to the results of Kaskan.

Shown in figure 9 is S_L as function of ϕ. Also shown are the experimental results of Law (1993), and the calculation results obtained with the 1-D flame code. It appears that our results are always lower (up to 4 cm/s) compared to the results of Law. However, as already mentioned in the introduction, in Law (1993) it is emphasized that to determine S_L by the opposed jet method, a linear extrapolation to zero strain rate has been

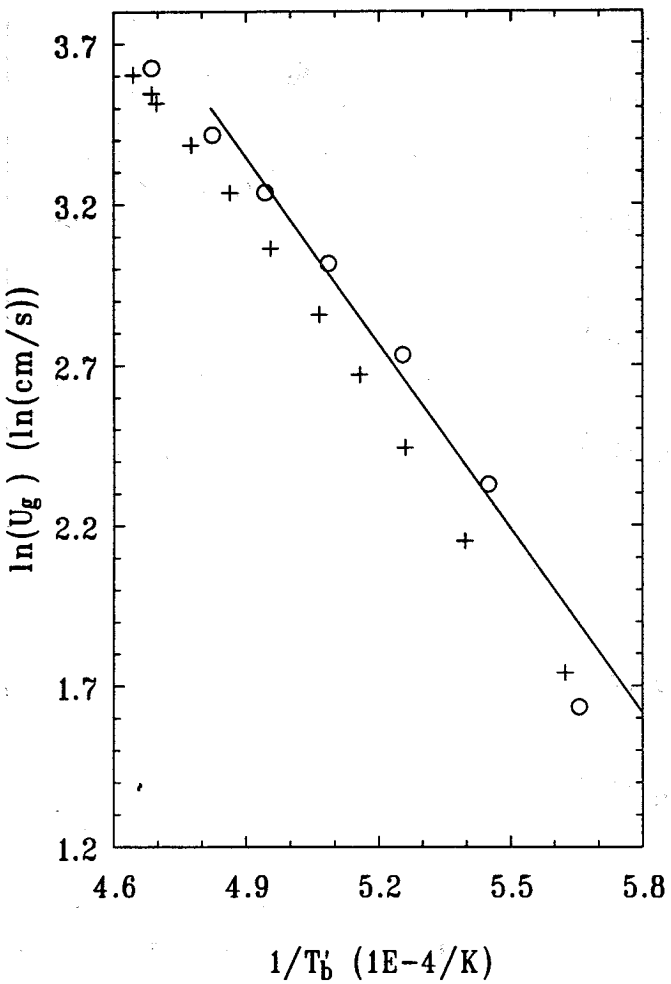

FIGURE 8 Flame temperature versus burning velocity for $\phi = 1.2$; cross markers: measurements, circle markers: calculations, continuous line: Kaskan (1959).

performed. Law states that this may result in adiabatic burning velocities which are too high (up to 10%). This probably explains the differences between our data and those of Law. Furthermore, Laser Doppler Velocimetry measurements in the flame have shown, that typical stretch rates in the flat flames were $O(1)\ s^{-1}$. Consequently, stretch effects in the flat flame results can be discarded. The results were reproducible within about 1-2 cm/s. Therefore we also come to the conclusion that the values for S_L obtained by Law are probably too high.

The differences between the experimental results for S_L and the 1-D flame calculations are probably caused by the choice of the chemical reaction rate coefficients. These differences in S_L can also explain the differences in T_b' in figures 6 to 8. Using the same values for T_b, but lower values for S_L, the experimental results for T_b' are shifted accordingly. Furthermore, the use of only a C_1 chemical reactions mechanism is possibly

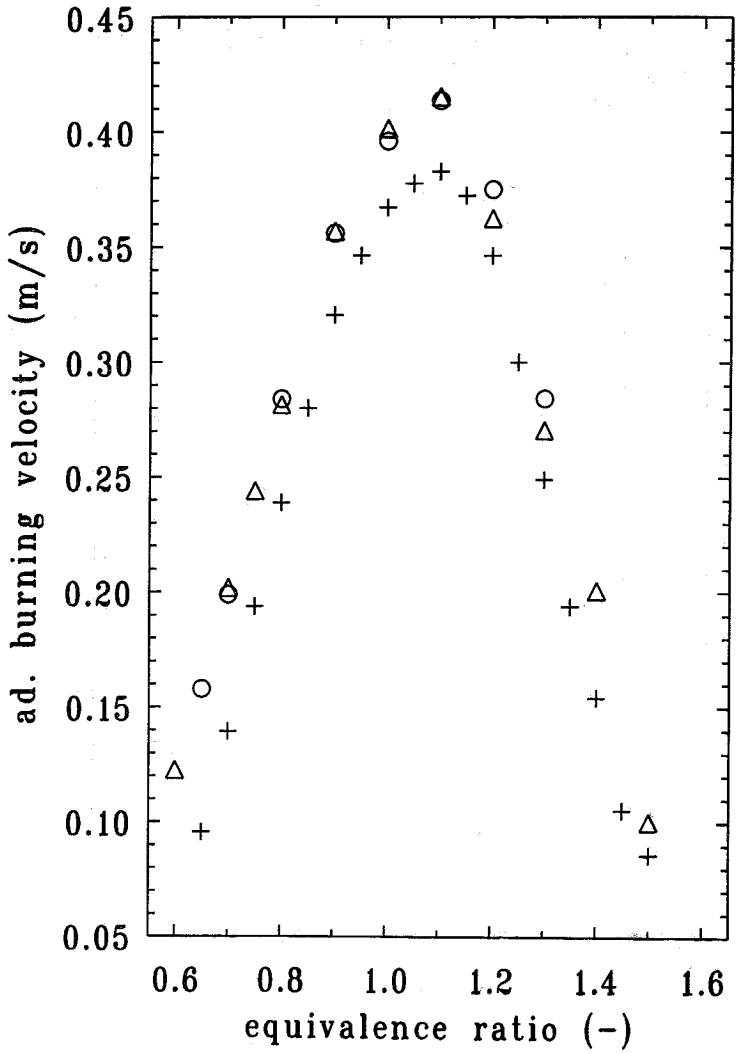

FIGURE 9 Adiabatic burning velocity versus equivalence ratio; cross markers: measurements, circle markers: calculations, triangle markers: Law (1993).

inadequate for near-stoichiometric and rich mixtures. In the near future comparison with C_2-mechanisms will be performed as well.

ERROR ESTIMATION

Adiabatic Burning Velocity

As S_L is found when the net heat loss is zero, the error in S_L is only dependent on the error in the Laser Doppler calibration of u_g (overall error less than 1%), the error in the mass flow controllers (0.5%) and in the equivalence ratio ($\lesssim$ 0.5%). This would imply an overall error in S_L of maximum 2%. However, as mentioned before, during the experiments it appeared that the results were reproducible within 1-2 cm/s.

Flame Temperature

The flame temperature T_b' is found by measuring the temperature difference $T_b - T_b'$. Therefore, for near-adiabatic flames the error in the calculation of T_b is dominant, being less than 1%. For larger values of $T_b - T_b'$ (e.g. 500 K) the error in the measured plate temperature (reproducible within 0.3 K) and in constants like ε, h and the exact location of the thermocouples prevails. Altogether an error of about 5% in $T_b - T_b'$ is found, yielding an error in T_b' of about 25-50 K.

CONCLUSIONS

A new method for determining the adiabatic burning velocity is presented, using a new type of flat flame burner. The method requires no correction for stretch or any extrapolation, like in the case of most conventional methods. However, the velocity results have to be corrected (with a maximum of 0.5 cm/s) by Laser Doppler Velocimetry measurements in the unburnt gas flow.

The method is applied to methane/air mixtures with varying equivalence ratio. Compared to experimental data of Law (1993) lower values are found (maximum 4 cm/s). It is shown that this may be caused by extrapolation errors in the experimental data of Law. Comparison with numerical calculations with detailed chemistry gives the same difference. This can be attributed to the fact that the coefficients of the chemical reaction scheme that is used are fitted with other, higher adiabatic burning velocity data.

With the same burner also flame temperatures have been determined. The accuracy is high, in particular near the adiabatic burning velocity. Taking into account the lower adiabatic burning velocities that are found, the presented results show good agreement with both experimental data found in the literature, and numerical calculations.

The method provides a well-defined flat flame with a well-known flame temperature and burning velocity, especially when operated in a near-adiabatic situation. This can be employed as a reference, for instance for spectroscopic laser diagnostics.

ACKNOWLEDGEMENT

The support of NOVEM and Gastec N.V., the Netherlands, is gratefully acknowledged. Also the authors would like to thank Dr. P. J. M. Sonnemans, who performed the numerical calculations of ε.

REFERENCES

Andrews, G. E., Bradley, D. (1972). The burning velocity of methane-air mixtures. *Combustion and Flame* **19,** 275.

Bird, R. B., Stewart, W. E., Lightfoot, E. N. (1960). *Transport Phenomena.* John Wiley & Sons, Inc., New York.

Bode, K. H., Fritz, W. (1958). New apparatus for measuring the thermal conductivities of metals. *Z Angew Phys* **10,** 470.

Botha, J. P., Spalding, D. B. (1954). The laminar flame speed of propane/air mixtures with heat extraction from the flame. *Proc Roy Soc Lond A,* **255,** 71.

Clarke, A., Stone, C. R., Beckwith, P. (1993). Measurement of laminar burning velocity in near zero gravity conditions. *Proceedings of the Anglo-German Combustion Symposium,* 231, Queens' College, Cambridge, UK, 29 March - 2 April.

De Goey, L. P. H., Van Maaren, A., Quax, R. M. (1993). Stabilization of adiabatic premixed laminar flames on a flat flame burner. *Combus. Sci. and Tech.* **92,** 1-3, 201

De Lange, H. C., De Goey, L. P. H. (1993). Two-dimensional methane/air flames. *Combus. Sci. and Tech.* **92,** 4-6, 423

DIN Taschenbuch 26 (1984). Beuth Verlag Gmbh, Berlin.

Eng, J. A., Egolfopoulos, F. N., Law, C. K. (1991). On the dual response and surface recombination in burner-stabilized flames, in *Heat Transfer in Fire and Combustion Systems,* HTD-Vol. 166, ASME 1991, 35.

Kaskan, W. E. (1959). The dependence of flame temperature on mass burning velocity. *Sixth Symposium (Int.) on Combustion,* 134, the Combustion Institute.

Kee, R. J. *et al.* (1986). Sandia Report SAND86-8246-UC-401. Sandia National Laboratories, Livermore, California 94551, U.S.A.

Kee, R. J. *et al.* (1987). Sandia Report SAND87-8215B-UC-4. Sandia National Laboratories, Livermore, California 94551, U.S.A.

Kee, R. J. *et al.* (1991). Sandia Report SAND85-8240-UC-401. Sandia National Laboratories, Livermore, California 94551, U.S.A.

Kihara, D. H., Fox, J. S., Kinoshita, C. M. (1975). Temperature and velocity non-uniformity in edge cooled flat flame burners. *Combus. Sci. and Tech.* **11,** 239.

Law, C. K. (1993). A compilation of experimental data on laminar burning velocities, in Peters, N., Rogg, B., (ed.'s), *Reduced kinetic mechanisms for applications in combustion systems,* Lecture Notes in Physics **19,** Springer Verlag, Berlin.

Lewis, B., Von Elbe, G. (1961). *Combustion, Flames and Explosion of gases, 2nd edition,* Academic Press.

Perrins, W. T., McKenzie, D. R., McPhedran, R. C. (1979). Transport properties of regular arrays of cylinders. *Proc Roy Soc Lond A,* **369,** 207.

Sonnemans, P. J. M. (1992). *Application of body-fitted coordinates in heat conduction problems* Ph.D. thesis, Eindhoven University of Technology, Eindhoven, the Netherlands.

Van Maaren, A., De Goey, L. P. H. (1993). Laser Doppler Thermometry in flat flames. *(submitted for publication to Combustion Science and Technology).*

Versluis, A. M. (1992). *Combustion diagnostics at atmospheric pressures using a tunable excimer laser.* Ph.D. thesis, Nijmegen University, Nijmegen, the Netherlands.

Warnatz, J., Chevalier, C. (1993). Critical survey of elementary reaction rate coefficients in the C/H/O system, in Gardiner jr., W. C. (ed.), *Combustion chemistry,* 2nd edition. Springer Verlag, New York (in preparation).

Wu, C. K, Law, C. K. (1984). On the determination of laminar flame speeds from stretched flames. *Twentieth Symposium (Int.) on Combustion,* 1941, the Combustion Institute.